

Optimality criteria based seismic design of multiple tuned-mass-dampers for the control of 3D irregular buildings

Yael Daniel¹ and Oren Lavan^{*2}

¹*Department of Civil Engineering, University of Toronto, Toronto, Canada*

²*Faculty of Civil and Environmental Engineering, Technion- Israel Institute of Technology, Haifa, Israel*

(Received February 26, 2014, Revised June 5, 2014, Accepted June 13, 2014)

Abstract. Multiple tuned mass dampers (MTMDs) tuned to various frequencies have been shown to efficiently control the seismic response of structures where multiple modes are dominant. One example is irregular structures that are found more vulnerable than their symmetric counterparts. With the technology of MTMDs available, design and optimal design methodologies are required for application. Such a methodology, in the form of an analysis/redesign (A/R) scheme, has been previously presented by the authors while limiting responses of interest to allowable values, i.e., performance-based design (PBD). In this paper, the A/R procedure is modified based on formal optimality criteria, making it more cost efficient, as well as more computationally efficient. It is shown that by using the methodology presented herein, a desired performance level is successfully targeted by adding near-optimal amounts of mass at various locations and tuning the TMDs to dampen several of the structure's frequencies. This is done using analysis tools only.

Keywords: irregular structures; multiple tuned mass dampers; multi modal control; seismic design of tall buildings; acceleration control

1. Introduction

Over the years, effort has been put into evaluating and understanding the seismic behavior of structures under seismic loading. In turn, effort has also been put in hopes of enhancing and controlling the seismic response so as to reduce resultant damage experienced by structures. This is true especially in the case of irregular or complex structures, that are often more vulnerable to these loads, due to their irregular nature. In recent years, the performance-based design (PBD) approach (e.g., Fajfar and Krawinkler 1997, Priestley 2000) has been adopted for seismic design of structures (FEMA 356). Here, structures are controlled and brought to behave within limits of desired performance, thus limiting the levels of damage (both structural and nonstructural) occurring to the structure following a seismic event. In addition to seismic threats, some structures may need to withstand forces created by other hazards, such as wind storms. These situations, often referred to as multi-hazard, relate to cases where a dynamic load of more than one source

*Corresponding author, Associate Professor, E-mail: lavan@tx.technion.ac.il

^aPostdoctoral Fellow

governs the design of the structure.

In recent decades, there has been a tendency of adding external control systems to enhance dynamic structural performance and allow the retrofit of existing structures. Control systems include passive and active damping, making use of dampers, and base-isolation systems. Herein, a passive control system utilizing Tuned-Mass Dampers (TMD) is chosen. TMDs have been shown to be able to eliminate most of the steady state motion of a linear single degree of freedom system under a harmonic loading of a given frequency, if properly tuned (e.g., Den-Hartog 1940, Warburton 1982, Bakre and Jangid 2007). TMDs have the advantage of their behavior being simple to model and their relatively low cost. TMDs have previously been very successfully implemented for reduction of vibrations due to wind storms (e.g., McNamara 1977, Luft 1979, Wiesner 1979), where a single fundamental mode usually excites the structure. Methods for the analysis of TMDs in torsionally coupled systems due to wind have been proposed (Pansare and Jangid 2003). An algorithm for the design of multiple active TMDs has been proposed for the control of flexural and torsional wind vibrations of tall structures as well (Venanzi *et al.* 2013). Therefore, if TMDs can be proven to be efficient also under seismic loadings (where multiple modes of the structure are often excited) they can be a very desirable control solution in the context of multi-hazard mitigation for seismic as well as wind loadings, as the same device can be used for both phenomena.

Using such TMDs for the seismic control of multi degree of freedom buildings with multiple modes contributing to their response is still limited, since each such damper is capable of successfully damping only a single mode of the structure. To overcome this obstacle, using several TMDs tuned to several modes of the structure was suggested (Clark, 1998). Seismic control of multi degree of freedom structures by means of TMDs and MTMDs (the latter referring to a case where the dampening of more than one mode in each direction is targeted) have been previously studied (e.g., Wirsching and Campbell 1974, Luft 1979, Jangid and Datta 1997, Sadek *et al.* 1997, Hadi and Arfiadi 1998, Lin *et al.* 1999, Schmitendorf 2000, Chen and Wu 2001, Lin *et al.* 2001, Singh *et al.* 2002, Ahlawat and Ramaswamy 2003, Zuo and Nayfeh 2004, Lee *et al.* 2006, Li and Qu 2006, Desu *et al.* 2006, Desu *et al.* 2007, Wang *et al.* 2009, Fu and Johnson 2009, Luo *et al.* 2009, Petti and De Iuliis 2009, Lin *et al.* 2010, Fu and Johnson 2011, Lin *et al.* 2011, Almazan *et al.* 2012). Different formulations and design methodologies are used to decide on the location and tuning properties of the dampers.

While the abovementioned studies present a huge step forward, a simple, practical, computationally efficient methodology for efficient PBD seismic retrofitting by means of MTMDs to control several modes is still lacking. The authors have recently presented a simple and practical PBD analysis/redesign procedure for the efficient allocation and sizing of multiple TMDs in 3D irregular structures (Lavan and Daniel 2013). This procedure is modified herein so as to make it more efficient, both cost-wise and computation-wise. Cost-wise efficiency is attained as the solutions obtained are closer to the actual optimal solution of the optimization problem considered. Computational efficiency is attained by avoiding evaluation of mean-square response at various frequencies, as required by the previous analysis/redesign procedure suggested. The first stage of redesign in the analysis/redesign algorithm includes redesign of the sum of masses of all TMDs at a specific location, based on the RMS response at that location. Thereafter, in the second stage of redesign, the masses of TMDs at the same location, tuned to various frequencies, are updated based on approximated gradients. Equal gradients were chosen to distribute the mass amongst TMDs at the same location so as to simulate a Karush-Kuhn-Tucker (KKT) solution (see for

example, Bazaraa and Shetty 1979) to the optimization problem, promising the solution will be near optimum. A full derivation of these KKT conditions is presented. Using the proposed methodology, a desired performance level is successfully targeted by adding near-optimal amounts of mass at various locations and tuning them to dampen several of the structure's frequencies. In addition, the proposed methodology is general, and therefore suitable for use in all types of structures, regardless of the extent of their irregularity, their shape or type.

2. Problem formulation

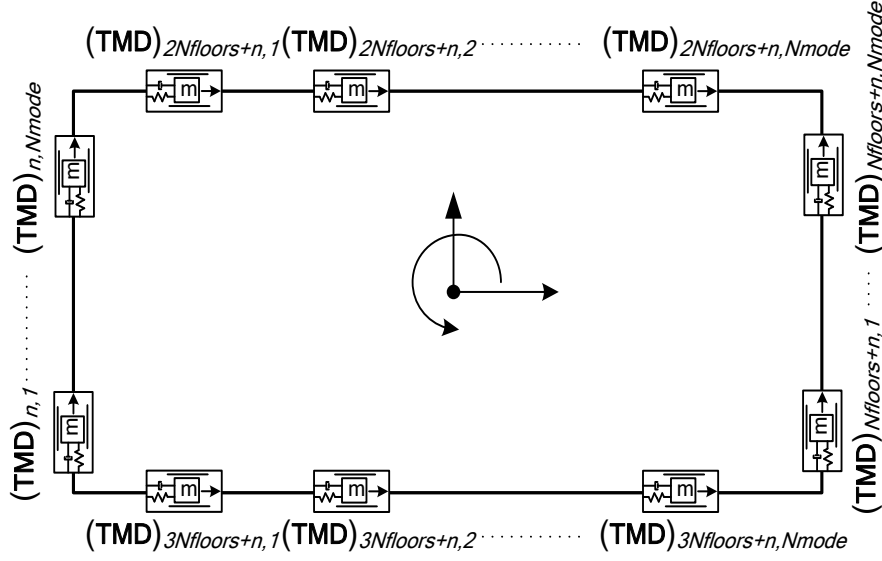
2.1 Performance measures

Structural control plays a key role in the PBD concept. To allow a desirable performance state, structural responses must often be limited so as to insure a prescribed maximal level of damage to structural, as well as nonstructural elements. When using TMDs in the context of multi-hazard mitigation, small drifts are expected within the structure during a ground motion. This is due to the large stiffness and strength of the structure required to withstand wind loads. In addition, wind effects are usually considerable in tall buildings that are often more slender. These will usually experience, under seismic loadings, smaller drifts than shorter buildings, and may not even yield (Priestley *et al.* 2007) as indeed was the case in the 2011 Tohoku earthquake (Kasai *et al.* 2012). Furthermore, drifts are reduced by the addition of TMDs even if those were not specifically considered as performance measures to be constrained. Thus, in the cases considered, drifts are assumed small and are, therefore, not directly dealt with herein. High acceleration at floor levels, on the other hand, may still be apparent under these seismic loads, especially in tall buildings (Kasai *et al.* 2012, Pu *et al.* 2012). Those responses are controlled and limited herein. High acceleration levels are often the cause of nonstructural damage, damage to sensitive equipment, as well as human discomfort. Reduction of those can also reduce base-shear forces and overturning moments (Soong and Dargush 1997, Chen and Wu 2001), and therefore may indirectly lead to smaller demands on force controlled elements as well. That is, control of acceleration levels leads to an overall better structural behavior, as well as smaller damage levels to nonstructural and force controlled structural elements.

To control accelerations, herein, TMDs are added to the structure. The cost of the control systems is determined based on the amount of added mass (this is through direct cost of material; void floor space for the control system, where as more mass is added, more valuable floor space is needed; and added gravitational forces to the existing structural system, which may lead to the need in strengthening those). As more mass is needed, the solution becomes more expensive, and therefore less cost-effective. Therefore, the sum of added masses is selected as the objective function to be minimized.

2.2 Problem formulation

The problem is formulated so as to try minimize control forces (masses of all dampers) while limiting RMS accelerations (stochastic representation of the seismic response in frequency domain) at peripheral locations to limits set by the performance criteria. Accelerations are limited at all peripheral locations of all floors, as they are the largest accelerations expected within the floor limits. Similarly, the TMDs are potentially located at peripheral locations, as these are the most

Fig. 1 Locations of TMDs at the floor n

efficient locations. At each location, several TMDs are potentially allocated, each tuned to a frequency corresponding to a different mode to be dampened (Fig. 1). The problem is formulated as

$$\min J = \sum_l^{\text{all locations}} \sum_f^{\text{all frequencies}} (\mathbf{m}_{\text{TMD}})_{l,f} \quad (1)$$

s.t.

$$\frac{RMS(\ddot{\mathbf{x}}_p^t)}{a_{\text{all}}^{\text{RMS}}} \leq 1.0 \quad \forall l = 1, 2, \dots, N_{\text{locations}}$$

where $(\mathbf{m}_{\text{TMD}})_{l,f}$ is the mass of the TMD located at peripheral location l tuned to frequency f of N_{mode} frequencies, $a_{\text{all}}^{\text{RMS}}$ is the allowable RMS total acceleration, $RMS(\ddot{\mathbf{x}}_p^t)$ is the root mean square of the total acceleration (noted t) at peripheral (noted p) location l (the l^{th} term of $RMS(\ddot{\mathbf{x}}_p^t)$), and $N_{\text{locations}}$ is the number of locations constrained ($=4N_{\text{floors}}$ where N_{floors} is the number of floors).

The problem is formulated as a linear-elastic problem since, as previously mentioned, smaller drifts are expected, and, therefore, it is assumed that no significant yielding occurs, and the structure behaves mostly linear and remains elastic. This allows the use of simplified and computationally efficient tools when solving the problem presented above. If yielding is expected, several measures could be used to accommodate that (see e.g., discussion at Lavan and Daniel (2013) and references therein).

3. Proposed solution scheme

Optimization problems of the type presented above have been solved using formal first-order, optimization schemes (Daniel and Lavan 2014), as has been proposed for the seismic design using other types of energy dissipation devices (e.g., Takewaki 1997, Takewaki 2000, Takewaki 2000b, Takewaki *et al.* 1999, Lavan and Levy 2005, Lavan and Levy 2006, Lavan and Amir 2014, Lavan and Levy 2010). Those, however, require knowledge and tools that are less familiar to practicing engineers. Optimality criteria methods have also been used in that context (e.g., Takewaki 1997, Levy and Lavan 2006, Lavan and Daniel 2013). Those could be roughly divided into formal optimality criteria that are based on KKT conditions (see e.g., Takewaki 1997) and intuitive optimality criteria (see e.g., Levy and Lavan 2006, Lavan and Daniel 2013). The solution scheme presented herein is a combination of intuitive optimality criteria for the distribution of the total mass of TMDs to the various locations, as those proposed by Lavan and Daniel (2013), and formal optimality criteria, for the determination of their tuning frequencies. It is of an analysis/redesign type and the attained designs satisfy the constraints while reducing the total mass of the MTMDs, thus achieving the goals of the performance based design. This procedure is expected to lead to a cost efficient solution that is close to the formal optimal one.

3.1 Optimality criteria based design

Optimality criteria methods could be roughly divided to two classes: Intuitive optimality criteria methods and more formal optimality criteria methods that are based on satisfying Karush-Kuhn-Tucker optimality conditions (see e.g., Haftka and Gurdal 1992). While, in general, the former methods may not lead to an optimum design, they are well known to lead to very efficient designs while requiring a limited number of iterations and make use of analysis tools only. The latter methods, on the other hand, do lead to local optimum. They require, however, the derivation of the gradients of the objective function and constraints.

Methods of the formal type have been used for the solution of seismic design using passive control devices. Takewaki (1997) tackled the problem of minimizing the sum of the amplitudes of the drifts' transfer functions evaluated at the undamped fundamental natural frequency of plane shear frames subject to a constraint on the total added viscous damping. He solved this optimization problem by using the optimality criteria he derived based on KKT conditions. The derivation of these conditions required the derivation of the gradients of the transfer functions of the inter-story drifts, evaluated at the undamped natural frequency of the structure, with respect to the damping vector.

Methods of the intuitive type have also been used in the context of seismic passive control. Levy and Lavan (2006) considered the minimization of total added viscous damping in frame structures subjected to ground accelerations while constraining inter-story responses. They indicated, based on formal optimal solutions attained elsewhere (Lavan and Levy 2005 2006), that: "*At the optimum, damping is assigned to stories for which the local performance index has reached the allowable value. Stories with no assigned damping attain a local performance index which is lower or equal to the allowable*". They further used their postulate to formulate a simple analysis/redesign type optimization scheme similar to that used for the solution of the truss of minimum weight that possesses Fully Stressed Design characteristics (Cilley 1900).

The authors have also proposed a full resources utilization design (FRUD) criteria for efficient

design of MTMDs in 3D irregular structures (Lavan and Daniel 2013). The FRUD criteria were stated as follows: *TMDs are assigned only to peripheral locations for which the RMS acceleration has reached the allowable value under the assumed Power-Spectral Density (PSD) of input acceleration. In addition, at each location where mass dampers are placed, TMDs of a given frequency are assigned only to frequencies for which the output spectral density is maximal.* When comparing the attained designs to formal optimal ones it was seen that while the first part of the statement holds in the optimal design, the second part, while leading to very efficient designs (close to optimal), does not lead to the true optimum. That is, while the intuitive optimality criterion formulated for the allocation of TMDs in space seems to hold, the question of how to distribute the mass between the various modes still remains.

In this paper, formal optimality criteria methods to distribute the mass at each location, between the various modes, are adopted. This leads to designs that are closer to optimum, while reducing the computational effort required (as more efficient frequency domain tools can be used). Using these optimality criteria, it is postulated that an efficient optimal, or close to optimal, selection of locations and sizes of MTMDs in structures, under a stochastic ground acceleration input, possesses the following characteristics: *TMDs are assigned to peripheral locations for which the RMS acceleration has reached the allowable value under the assumed PSD of input acceleration. In addition, at each location to which TMDs are added, TMDs of a given frequency are assigned only to frequencies for which the gradient of the RMS response at that location with respect to the mass of TMD that mode is set to dampen is most negative.* As indicated, the second part of this statement is based on optimality criteria methods that are aimed at satisfying the KKT conditions for optimum solutions (see e.g., Bazaraa and Shetty 1979). An explanation how the second part of the statement represents the KKT conditions can be found in Appendix A. For this derivation, an assumption on the KKT conditions is made- that only one constraint is active at the optimum (i.e., response at a single location). While this assumption may not always hold, it seems to lead to results that are close to the optimum, even when more constraints are active. Furthermore, approximated gradients are derived (see Appendix B for derivation, the final formula will be given in Section 4, Step 4, Stage 2). This allows the use of the method by engineers while using simple formulae rather than having to derive the gradients.

3.2 Analysis/redesign algorithm

Solutions to problems, which possess optimality criteria characteristics, as the ones postulated above, are efficiently achieved iteratively using a two step algorithm in each iteration cycle (see e.g., Cilley 1900, Haftka and Gurdal 1992). In the first step an analysis is performed for a given preliminary design, whereas in the second step the design is changed using a recurrence relationship that targets satisfaction of the optimality criterion. The recurrence relation can be generally written as

$$x_l^{(n+1)} = x_l^{(n)} \cdot \left(\frac{pi_l^{(n)}}{pi_{allowable}} \right)^P \quad (2)$$

where x_l is the value of the design variable associated with the location l , pi_l is the performance measure of interest for the location l , $pi_{allowable}$ is the allowable value for the performance measure, n - the iteration number and P - a convergence parameter. The advantages of the analysis/redesign

algorithm include its simplicity, the need to use analysis tools only, and the fairly small computational effort that lies in the small number of analyses required for convergence. Such analysis/redesign procedure will be utilized here to attain designs where the mass, frequency and locations of MTMDs within framed structures is to be determined, while satisfying both optimality criteria presented above.

4. Design methodology

Step 1: An allowable RMS acceleration is chosen. The mass, damping and stiffness matrices of the structure are assembled according to the relevant dynamic Degrees-of-Freedom (DOFs). Solution of the eigenvalue problem determines the structure's natural frequencies and mode shapes. A power spectral density (PSD), $S(\omega)$, for the input acceleration is chosen (e.g., white-noise, which gives a constant PSD; Clough-Penzien filtered Kanai-Tajimi PSD (Clough and Penzien 1995) etc.). RMS accelerations under the chosen input PSD are computed for each of the structure's DOFs (e.g., using Lyapunov's equation, see e.g., Kwakernaak and Sivan 1972), and then transformed to peripheral coordinates.

Step 2: If for any peripheral coordinate, l , the RMS acceleration obtained is larger than the allowable RMS acceleration, MTMDs are added to suppress the acceleration produced. Each TMD of mass $(\mathbf{m}_{\text{TMD}})_{l,f}$ is assigned with a DOF for its displacement relative to the ground. At each location, N_{mode} TMDs are potentially added, to suppress N_{mode} original frequencies of the structure.

The response of each mode could be evaluated based on a Single Degree-of-Freedom (SDOF) equivalent system. For the sake of simplicity, in this work Den-Hartog (1940) / Warburton (1982) properties were chosen. Nonetheless, more advanced criteria could easily be used with the proposed methodology (see e.g., Bakre and Jangid 2007). In the case of optimal Den-Hartog properties the following initial properties are taken for the dampers:

1. For each peripheral coordinate, the initial mass of all TMDs located at that coordinate is taken as certain predetermined percentage of the structure's mass (say 1%). It is divided equally between the dampers situated at the same location

$$(\mathbf{m}_{\text{TMD}})_{l,f} = (0.01 \cdot M_{structure}) / N_{mode} \quad (3)$$

where l represents the damper's location, f represents the mode dampened and $M_{structure}$ is the structure's total mass. The mass ratio $(\boldsymbol{\mu}_{\text{TMD}})_f$ of all TMDs tuned to frequency f is calculated as the ratio between the effective TMD mass of all TMDs tuned to frequency f and the f^{th} modal mass of the structure. This mass ratio is defined as

$$(\boldsymbol{\mu}_{\text{TMD}})_f = (\boldsymbol{\phi}_f^T \cdot \mathbf{T}^T \cdot \mathcal{D}((\mathbf{m}_{\text{TMD}})_f) \cdot \mathbf{T} \cdot \boldsymbol{\phi}_f) / (\boldsymbol{\phi}_f^T \cdot \mathbf{M}_{\text{original}} \cdot \boldsymbol{\phi}_f) \quad (4)$$

where $\boldsymbol{\phi}_f$ is the f^{th} mode-shape of the bare structure, $[\mathbf{M}_{\text{original}}]$ is the bare frame's mass matrix, \mathbf{T} is the transformation matrix to peripheral locations, and $\mathcal{D}((\mathbf{m}_{\text{TMD}})_f)$ is a diagonal matrix with

the terms $(\mathbf{m}_{\text{TMD}})_{1:N_{\text{locations}}f}$ sitting on the diagonal.

2. Each TMD's stiffness is determined according to the frequency of the mode which is damped by the TMD. The frequency is tuned to

$$(\boldsymbol{\omega}_{\text{TMD}})_f = (\boldsymbol{\omega}_n)_f / (1 + (\boldsymbol{\mu}_{\text{TMD}})_f) \quad (5)$$

where $(\boldsymbol{\omega}_n)_f$ is the frequency f to be damped. The compatible stiffness is

$$(\mathbf{k}_{\text{TMD}})_{l,f} = (\mathbf{m}_{\text{TMD}})_{l,f} \cdot ((\boldsymbol{\omega}_{\text{TMD}})_f)^2 \quad (6)$$

3. Each TMD's damping ratio is determined according to

$$(\boldsymbol{\xi}_{\text{TMD}})_f = \sqrt{(3 \cdot (\boldsymbol{\mu}_{\text{TMD}})_f) / (8 \cdot (1 + (\boldsymbol{\mu}_{\text{TMD}})_f)^3)} \quad (7)$$

and the matching damping coefficient

$$(\mathbf{c}_{\text{TMD}})_{l,f} = 2 \cdot (\mathbf{m}_{\text{TMD}})_{l,f} \cdot (\boldsymbol{\xi}_{\text{TMD}})_f \cdot (\boldsymbol{\omega}_n)_f \quad (8)$$

Step 3: The mass, damping and stiffness matrices of the damped frame are updated. Peripheral RMS accelerations are then reevaluated.

Step 4: TMD's masses are re-determined using two stages; the total mass of all dampers located at a given location is first determined. This is followed by the distribution of that mass between all TMDs at that location, having various tuning frequencies. Following the change in mass, the stiffness and damping ratio of each TMD are also updated while keeping the Den-Hartog principles intact, using Eqs. (5) - (8). This leads to the optimal stiffnesses and damping ratios of the TMDs in each iteration and eliminates some possible effects of the initial design on the final one. The two-stage analysis/redesign procedure is carried out iteratively until convergence, in the following way:

Stage 1: The first stage of redesign includes evaluation of the total mass of TMDs at each location, promising the existence of the first part of the postulate. This is formulated using

$$(\mathbf{m}_{\text{TMD, total}}^{(n+1)})_l = \sum_{f=1}^{\text{all frequencies}} (\mathbf{m}_{\text{TMD}}^{(n+1)})_{l,f} = \sum_{f=1}^{\text{all frequencies}} (\mathbf{m}_{\text{TMD}}^{(n)})_{l,f} \cdot \left(\frac{\text{RMS} \left(\left(\ddot{\mathbf{x}}_p^t \right)_l^{(n)} \right)}{a_{\text{all}}^{\text{RMS}}} \right)^P \quad (9)$$

where $(\cdot)^{(n)}$ is the value at iteration n , $(\mathbf{m}_{\text{TMD, total}}^{(n+1)})_l$ is the total mass of all dampers at location l , and P is a constant which influences the convergence and convergence rate. A large P will result in a faster but less stable convergence of the above equation. Based on the authors' experience, a P in the range of 0.1-2.0 should be satisfying in terms of stability, convergence and fair amount of iterations.

Stage 2: In the second stage of redesign, the total mass obtained at each location is distributed between N_{mode} dampers (dampening modes $(\boldsymbol{\omega}_n)_f$) at that same location l , promising the existence of the second part of the postulate, using the following

$$\left(\mathbf{m}_{\text{TMD}}^{(n+1)}\right)_{l,f} = \left(\mathbf{m}_{\text{TMD}}^{(n)}\right)_{l,f} \left(\frac{\frac{\partial \left(\text{RMS} \left(\left(\ddot{\mathbf{x}}_p^t \right)_l^{(n)} \right) \right)}{\partial \left(\mathbf{m}_{\text{TMD}} \right)_{l,f}}}{\max_f \left(\frac{\partial \left(\text{RMS} \left(\left(\ddot{\mathbf{x}}_p^t \right)_l^{(n)} \right) \right)}{\partial \left(\mathbf{m}_{\text{TMD}} \right)_{l,f}} \right)} \right)^P \cdot NF \quad (10)$$

and

$$NF = \frac{\left(\mathbf{m}_{\text{TMD, total}}^{(n+1)}\right)_l}{\sum_{f=1}^{\text{all frequencies}} \left(\mathbf{m}_{\text{TMD}}^{(n)}\right)_{l,f} \left(\frac{\frac{\partial \left(\text{RMS} \left(\left(\ddot{\mathbf{x}}_p^t \right)_l^{(n)} \right) \right)}{\partial \left(\mathbf{m}_{\text{TMD}} \right)_{l,f}}}{\max_f \left(\frac{\partial \left(\text{RMS} \left(\left(\ddot{\mathbf{x}}_p^t \right)_l^{(n)} \right) \right)}{\partial \left(\mathbf{m}_{\text{TMD}} \right)_{l,f}} \right)} \right)^P} \quad (11)$$

where the approximated gradient $\frac{\partial \left(\text{RMS} \left(\left(\ddot{\mathbf{x}}_p^t \right)_l^{(n)} \right) \right)}{\partial \left(\mathbf{m}_{\text{TMD}} \right)_{l,f}}$ is evaluated based on the following equation (see Appendix B for derivation of this expression)

$$\frac{\partial \left(\text{RMS} \left(\left(\ddot{\mathbf{x}}_p^t \right)_l^{(n)} \right) \right)}{\partial \left(\mathbf{m}_{\text{TMD}} \right)_{l,f}} \approx \frac{\left(\mathbf{T} \cdot \phi_f \right)_l^2 \cdot \Gamma_f^2}{\text{RMS} \left(\left(\ddot{\mathbf{x}}_p^t \right)_l^{(n)} \right)} \cdot \frac{\phi_f^T \mathbf{B}_d^T}{\phi_f^T \cdot \mathbf{M}_{\text{original}} \cdot \phi_f} \cdot \frac{\frac{\partial \mathcal{D}(\mathbf{m})}{\partial \left(\mathbf{m}_{\text{TMD}} \right)_{l,f}} \cdot \mathbf{B}_d \phi_f}{\partial \left(\boldsymbol{\mu}_{\text{TMD}} \right)_f} \cdot \frac{\partial \left(MS \left(\left(\ddot{\mathbf{x}}_p^t \left(\omega_f \right)^{(n)} \right)_{\max} \right) \right)}{\partial \left(\boldsymbol{\mu}_{\text{TMD}} \right)_f} \quad (12)$$

where the matrix \mathbf{B}_d is a transformation matrix, used to assign the TMDs within the structure, Γ_f is the participation factor of mode f , defined as $\Gamma_f = \frac{\phi_f^T \cdot \mathbf{M}_{\text{original}} \cdot \mathbf{e}_s}{\phi_f^T \cdot \mathbf{M}_{\text{original}} \cdot \phi_f}$ where \mathbf{e}_s is the excitation direction vector with values of zero and one for DOFs perpendicular and parallel to the excitation direction, respectively, and the gradient $\frac{\partial \left(MS \left(\left(\ddot{\mathbf{x}}_p^t \left(\omega_f \right)^{(n)} \right)_{\max} \right) \right)}{\partial \left(\boldsymbol{\mu}_{\text{TMD}} \right)_f}$ is derived based on an

empirical formula obtained using curve-fitting, and is

$$\frac{\partial \left(MS \left(\left(\ddot{\mathbf{x}}_p^t \left(\omega_f \right)^{(n)} \right)_{\max} \right) \right)}{\partial \left(\boldsymbol{\mu}_{\text{TMD}} \right)_f} = -3.15099 \cdot \left(\left(\boldsymbol{\mu}_{\text{TMD}} \right)_f + 0.003 \right)^{-1.12041} \cdot \left(\left(\boldsymbol{\omega}_n \right)_f \right)^{0.5} \cdot S \left(\left(\boldsymbol{\omega}_n \right)_f \right) \quad (13)$$

where $S \left(\left(\boldsymbol{\omega}_n \right)_f \right)$ is the value of the input PSD $S(\omega)$ at the frequency $\omega = \left(\boldsymbol{\omega}_n \right)_f$.

In deriving the approximated gradient *only*, it was assumed that, approximately, the equations of motion of the damped structure are not coupled when transformed to the modal coordinates of

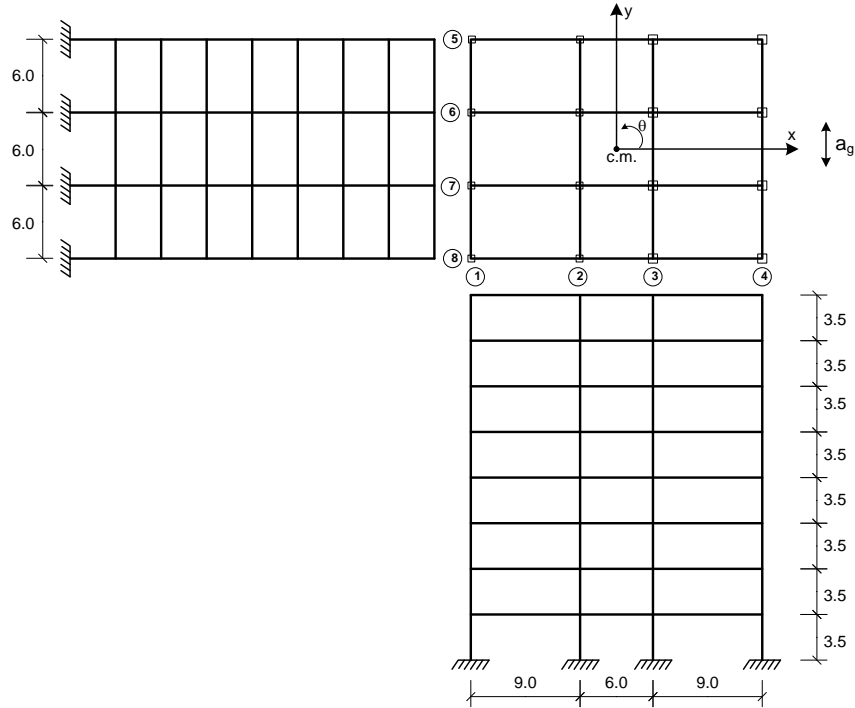


Fig. 2 Eight-story asymmetric structure

the undamped structure, and that the TMDs tuned to dampen a certain mode do not affect the response of other modes. It should be noted that when assessing structural responses during the analysis stage, the full uncoupled equations of motion are considered. Therefore, this assumption only affects the optimality of the design in terms of the total added mass, and does not cause violation of the constraints. As will be seen in the examples, the solutions attained by the proposed strategy are very close to the formal optimal solution, i.e., the abovementioned assumption is acceptable in this context. In addition, for this approximated gradient, the forces in TMDs due to the ground's movement are neglected, and it is assumed that forces in all TMDs are created only due to the structure's movement.

Step 5: Repeat steps 3-4 until convergence of the mass is reached.

4. Example

The following 8-story asymmetric RC frame structure (Fig. 2) introduced by Tso and Yao (1994) is retrofitted using MTMDs for a deterministic ensemble of ground motions exciting the structure in the “y” direction). A uniform distributed mass of 0.75 ton/m^2 is taken. The column dimensions are 0.5 m by 0.5 m for frames 1 and 2 and 0.7 m by 0.7 m for frames 3 and 4. The beams are 0.4 m wide and 0.6 m tall. 5% Rayleigh damping for the first and second modes is used. A 40% reduction of the RMS total acceleration in the bare structure is desired. The response is

analyzed under a Clough-Penzien filtered Kanai-Tajimi PSD with parameters fitted to the average FFT values of the SE10/50 ground-motion ensemble. The design variables are the locations and properties of the individual tuned mass dampers. The dampers are to potentially be located in the peripheral frames, where they are most effective, and as the excitation is in the “y” direction only, dampers will be assigned only to the peripheral frames 1 and 4, to dampen frequencies of modes which involve “y” and “ θ ”.

Step 1: The mass, inherent damping and stiffness matrices of the frame in the dynamic DOFs were constructed. The natural frequencies, of the structure were determined. The first 10 modes are: 5.14s (x), 5.46s (y, θ), 7.09s (y, θ), 16.24s (x), 16.94s (y, θ), 22.41s (y, θ), 29.65s (x), 29.88s (y, θ), 43.8440.92s (y, θ), 44.77s (y, θ). RMS accelerations of the undamped structure are evaluated under the Clough-Penzien filtered Kanai-Tajimi PSD with parameters: $\omega_g = 13 \text{ rad/sec}$, $\xi_g = 0.98$, $S_0 = 1$, $\omega_f = 1.5 \text{ rad/sec}$, and $\xi_f = 0.9$. These parameters were computed such that the attained PSD fits best the PSD of the SE 10/50 ground motion ensemble (see Lavan and Daniel 2013). The allowable RMS acceleration for all peripheral accelerations was earlier adopted as 60% of the maximum peripheral RMS acceleration of the bare frame, giving: $a_{\text{all}}^{\text{RMS}} = 15.28$.

Step 2: 160 TMDs were added, as a first guess, with initial properties as given in Table 1. Those are comprised of 10 dampers each tuned to a different mode frequency (of modes related to “y” and “ θ ”) at each of the 16 peripheral locations of frames 1 and frame 4.

Step 3: The mass, stiffness and damping matrices were updated. With the newly-updated matrices and the same PSD input, new peripheral RMS accelerations were evaluated. Some of the peripheral accelerations in frames 1 and 4 exceeded the allowable.

Table 1 Initial properties of TMDs

No. TMD	Mode to dampen	Initial mass (ton)	Initial natural frequency (rad/sec)	Initial damping ratio
1-16	2	2.592	5.37	0.0788
17-32	3	2.592	6.89	0.1004
33-48	5	2.592	16.64	0.0795
49-64	6	2.592	21.78	0.0998
65-80	8	2.592	29.34	0.0805
81-96	9	2.592	39.79	0.0989
97-112	10	2.592	43.94	0.0816
113-128	12	2.592	60.28	0.0822
129-144	13	2.592	62.30	0.0983
145-160	15	2.592	77.55	0.0826

Table 2 Final properties of added TMDs

Frame	Floor	Mode to dampen	Final mass (ton)	Final stiffness (kN/m)	Final damping ratio
1	8	2	86.89	2040.89	0.1825
1	8	5	18.93	5138.92	0.0981
1	8	8	3.95	3491.48	0.0447
4	8	3	1.74	58.69	0.0304

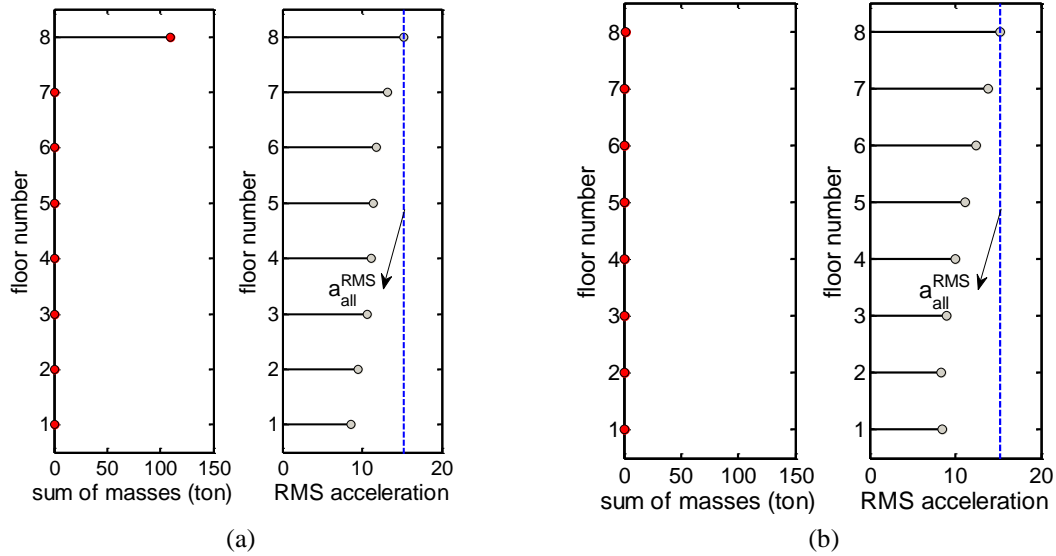


Fig. 3 Peripheral RMS accelerations of structure with final TMDs (continuous) and sum of added masses (dots) (a) frame 1 and (b) frame 4

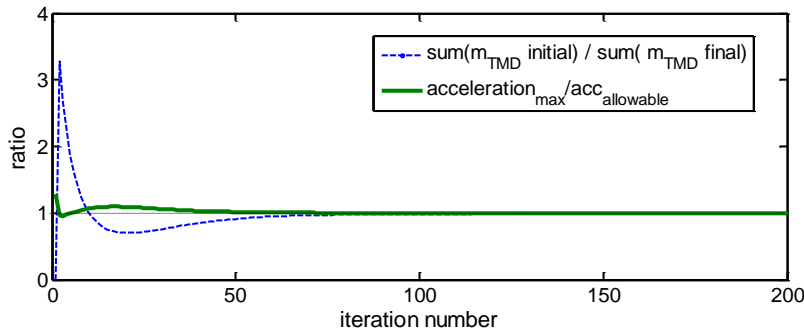


Fig. 4 Convergence of normalized sum of masses (objective function) and maximum normalized RMS acceleration (constraint)

Step 4: The problem has not converged, and thus the TMDs' properties were altered, using the recurrence relations of Eqs. (9) - (11) and $P=0.5$ as the convergence parameter, giving updated total masses at each DOF. The total mass of each peripheral coordinate was then distributed between the 10 dampers at the same location using Eqs. (10) and (11). Iterative analysis/redesign as described in Eqs. (9) - (11) while altering the mass of the damper is carried out until convergence to allowable levels. Upon convergence, the mass of added dampers are shown in Table 2. TMDs with non-zero properties were located at the 8th floors of frame number 1 and number 4. The final properties of each added TMD are shown in Table 2. All assigned TMDs add up to 4.28% of the original structure's mass. For all practical reasons, TMDs with small masses can be neglected without effecting the response of the structure.

Finally, an analysis of the retrofitted structure yields the peripheral RMS accelerations shown

Table 3 Results comparison

	% added mass	Number of iterations/ function evaluations*	Computational time (sec)
Formal optimal solution	4.00%	~70	~2400
A/R frequency response	4.59%	~40	~600
A/R approximated gradient	4.28%	~60	~60

* Note that as different tools are used in each methodology computational effort cannot be compared directly.

in Fig. 3. Also in Fig. 3 the total amount of mass at each floor is shown. As can be seen, only locations who had reached the maximum allowable RMS total acceleration were assigned with added absorbers, making the solution obtained a fully-stressed design.

Fig. 4 presents the convergence of the design variables (masses) and the performance measure (acceleration). As can be seen in Fig. 3, full convergence is reached within about 150 iterations (although practically only 60 iterations are required). In the evolution of the solution, it could be observed that the algorithm first increases the mass considerably so as to satisfy the acceleration constraints (first 5 iterations or so). Then, efforts are made to keep satisfying the constraints while significantly minimizing the mass. Monotonic convergence is achieved once the solution reaches the vicinity of the optimal design, i.e. from iteration 15 or so and on. It should be noted that the same final solution was attained using various initial designs (TMD properties). That is, the analysis/redesign algorithm presented herein is stable and is insensitive to random choices of the engineer to use it, including the initial guess. Although the problem at hand does not seem to be convex the fact that the same solution was attained while starting from various initial designs indicates that, with a high probability, the attained solution is the global one.

The results attained were compared to results attained using formal optimization (Daniel and Lavan 2014) and the previous analysis/redesign-based methodology presented by the authors (Daniel and Lavan 2011), and are presented in Table 3. Note that the number of iterations/function evaluations needed is given for comparison-of-convergence-sake, however, as different tools are used in each methodology (formal optimization tools with sensitivities in the first, frequency response analysis at all frequencies in the second, and approximated gradient without full frequency analysis in the third), computational effort cannot be compared directly, and therefore computational time is also given, to help better estimate computation effort.

6. Conclusions

A performance-based methodology for the retrofitting of 3D irregular structures was presented. This methodology makes use of an iterative two-step analysis/redesign procedure to limit RMS absolute acceleration levels at all peripheral locations to an allowable level. A previous methodology for solution of the same problem was previously presented by the authors. It used a similar analysis/redesign procedure that was based on an equal frequency responses of modes associated with TMDs dampening them for the second stage of the redesign step. This led to a solution that was based on analysis tools only, and was fast-converging, but the results were only close to optimal (compared to the formal optimal solution of the problem). Herein, a different

variation on the analysis/redesign method was suggested, so as to still only use analysis tools, but based on a modified refined criteria for the second stage of the redesign step, that is based on optimality conditions. This approach, while still fast converging, led to results that were closer to the optimal results than the first analysis/redesign methodology used. In addition, thanks to the approximated expression of the gradient, and its use in the second stage of the redesign step, full frequency analysis is not needed in this analysis/redesign variation, as opposed to the one originally suggested, making the proposed methodology even more computationally efficient.

Results showed that MTMDs can be used for seismic design of structures, and that those can reduce accelerations to a desired level. TMDs tuned to several modes and located in different peripheral locations are utilized to obtain effectiveness. The results obtained were indeed close to the optimal solution of the problem, as was shown. A similar trend was observed in other examples as well (e.g., Daniel and Lavan 2013). The advantages of the design methodology presented herein include its simplicity, relying on analysis tools only, its fast convergence, its generality and suitability to many problems, regardless of irregularities, all of which make it applicable for use in practical design.

References

- Ahlawat, A.S. and Ramaswamy, A. (2003), "Multiobjective optimal absorber system for torsionally coupled seismically excited structures", *Eng. Struct.*, **25**, 941-950.
- Almazan, J.L. Espinoza, G. and Aguirre, J.J. (2012), "Torsional balance of asymmetric structures by means of tuned mass dampers", *Eng. Struct.*, **42**, 308-328.
- Bakre, S.V. and Jangid, R.S. (2007), "Optimum parameters of tuned mass damper for damped main system", *Struct. Control Health Monit.*, **14**, 448-470.
- Bazaraa, M.S. and Shetty, C.M. (1979), *Nonlinear programming. Theory and algorithms*, John Wiley & Sons.
- Chen, G. and Wu, J. (2001), "Optimal placement of multiple tune mass dampers for seismic structures", *ASCE J. Struct. Eng.*, **127**(9), 1054-1062.
- Cilley, F.H. (1900), "The exact design of statically indeterminate frameworks, an exposition of its possibility but futility", *ASCE, Transact.*, **43**, 353-407.
- Clark, A.J. (1988), "Multiple passive tuned mass dampers for reducing earthquake induced building motion", *Proceedings of the 9th World Conference on Earthquake Engineering*, Tokyo-Kyoto, Japan.
- Clough, R.W. and Penzien, J. (1995), *Dynamics of Structures*, 3rd Edition, Computers & Structures, Inc.
- Daniel, Y. and Lavan, O. (2011), "Seismic design methodology for control of 3D buildings by means of multiple tuned-mass-dampers", *Computational Methods in Structural Dynamics and Earthquake Engineering (COMPdyn 2011)*, Island of Corfu, Greece, May 2011, Paper No. 147.
- Daniel, Y. and Lavan, O. (2013), "Approximated gradient based seismic control of 3D irregular buildings using multiple tuned-mass-dampers", *World Congress on Advances in Structural Engineering and Mechanics (ASEM13)*, Island of Jeju, Korea, September.
- Daniel, Y. and Lavan, O. (2014), "Gradient based optimal seismic retrofitting of 3D irregular buildings using multiple tuned mass dampers", *Comput. Struct.*, **139**, 84-97..
- Den-Hartog, J.P. (1940), *Mechanical Vibrations*, 2nd Edition, McGraw-Hill Book Company, Inc..
- Desu, N.B., Deb, S.K. and Dutta, A. (2006), "Coupled tuned mass dampers for control of coupled vibrations in asymmetric buildings", *Struct. Control Hlth. Monit.*, **13**, 897-916.
- Desu, N.B., Dutta, A. and Deb, S.K. (2007), "Optimal assessment and location of tuned mass dampers for seismic response control of a plan-asymmetric building", *Struct. Eng. Mech.*, **26**(4), 459-477.
- Fajfar, P. and Krawinkler, H. (1997), *Seismic Design Methodologies for the Next Generation of Codes*,

- Balkema, Rotterdam, 1997.
- FEMA 356 (2000), *Pre-standard and Commentary for the Seismic Rehabilitation Buildings*, Federal Emergency Management Agency, Washington DC.
- Fu, T.S. and Johnson, E.A. (2009), "Control strategies for a distributed mass damper system", *Proceedings of the American Control Conference*, St. Louis, MO, USA, June.
- Fu, T.S. and Johnson, E.A. (2011), "Distributed mass damper system for integrating structural and environmental control in buildings", *J. Eng. Mech.*, **137**(3) 205-213.
- Hadi, M.N.S. and Arfiadi, Y. (1998), "Optimum design of absorber for MDOF structures", *J. Struct. Eng.*, **124**(11), 1272-1280.
- Haftka R.T. and Gurdal, Z. (1992), *Elements of Structural Optimization*, 3rd Edition, Dordrecht, Kluwer Academic.
- Jangid, R.S. and Datta, T.K. (1997), "Performance of multiple tuned mass dampers for Torsionally coupled system", *Earthq. Eng. Struct. Dyn.*, **26**, 307-317.
- Kasai, K., Pu, W. and Wada, A. (2012), "Response of passively-controlled tall buildings in Tokyo during 2011 Great East Japan Earthquake", *Proceedings of the 15th World Conference on Earthquake Engineering*, Lisbon, Portugal.
- Kwakernaak, H. and Sivan, R. (1972), *Linear Optimal Control Systems*, John Wiley & Sons, Inc.
- Lavan, O. and Amir, O. (2014), "Simultaneous topology and sizing optimization of viscous dampers in seismic retrofitting of 3D irregular frame structures", *Earthq. Eng. Struct. Dyn.*, **43**(9), 1325-1342.
- Lavan, O. and Daniel, Y. (2013), "Full resources utilization seismic design of irregular structures using multiple tuned mass dampers", *J. Struct. Multidiscip. O.*, **43**(3), 517-532.
- Lavan, O. and Levy, R. (2005), "Optimal design of supplemental viscous dampers for irregular shear-frames in the presence of yielding", *Earthq. Eng. Struct. Dyn.*, **34**, 889-907.
- Lavan, O. and Levy, R. (2006), "Optimal peripheral drift control of 3D irregular framed structures using supplemental viscous dampers", *J. Earthq. Eng.*, **10**, 903-923.
- Lavan, O. and Levy, R. (2010), "Performance based optimal seismic retrofitting of yielding plane frames using added viscous damping", *Earthq. Struct.*, **1**, 307-326.
- Levy, R. and Lavan, O. (2006), "Fully stressed design of passive controllers in framed structures for seismic loadings", *J. Struct. Multidiscip. O.*, **32**, 485-498.
- Lee, C.L., Chen, Y.T., Chung, L.L. and Wang, Y.P. (2006), "Optimal design theories and applications of tuned mass dampers", *Eng. Struct.*, **28**, 43-53.
- Li, C. and Qu, W. (2006), "Optimum properties of multiple tuned mass dampers for reduction of translational and torsional response of structures subject to ground acceleration", *Eng. Struct.*, **28**, 472-494.
- Lin, C.C., Ueng, J.M. and Huang, T.C. (1999), "Seismic response reduction of irregular buildings using passive tuned mass dampers", *Eng. Struct.*, **22**, 513-524.
- Lin, C.C., Wang, J.F. and Ueng, J.M. (2001), "Vibration control of identification of seismically excited MDOF structure- PTMD systems", *J. Sound Vib.*, **240**(1), 87-115.
- Lin, J.L., Tsai, K.C. and Yu, Y.J. (2010), "Coupled tuned mass dampers for the seismic control of asymmetric-plan buildings", *Earthq. Spectra*, **26**(3), 749-778.
- Lin, J.L., Tsai, K.C. and Yu, Y.J. (2011), "Bi-directional coupled tuned mass dampers for the seismic response control of two-way asymmetric-plan buildings", *Earthq. Eng. Struct. Dyn.*, **40**, 675-690.
- Luft, R.W. (1979), "Optimum tuned mass dampers for buildings", *ASCE J. Struct. Div.*, **105**, 2766-2772.
- Luo, X., Ma, R., Li, G. and Zhao, D. (2009), "Parameter optimization of multi-mode vibration control system", *International Conference of Measuring Technology and Mechatronics Automation*, IEEE Computer Society, 685-688.
- McNamara, R.J. (1997), "Tuned mass dampers for buildings", *ASCE J. Struct. Div.*, **103**, 1785-1798.
- Pansare, A.P. and Jangid, R.S. (2003), "Tuned mass dampers for torsionally coupled systems", *Wind Struct.*, **6**, 23-40.
- Petti, L. and De Iuliis, M. (2009), "Robust design of a single tuned mass damper for controlling torsional

- response of asymmetric-plan systems”, *J. Earthq. Eng.*, **13**, 108-128.
- Priestley, M.J.N. (2000), “Performance based seismic design”, *Proceedings of the 12th World Conference on Earthquake Engineering*, Paper no. 2831.
- Priestley, M.J.N., Calvi, M.C. and Kowalsky, M.J. (2007), *Displacement-Based Seismic Design of Structures*, IUSS Press, Pavia.
- Pu, W., Kasai, K. and Kashima, T. (2012), “Response of conventional seismic-resistant tall buildings in Tokyo during 2011 great East Japan earthquake”, *Proceedings of the 15th World Conference on Earthquake Engineering*, Lisbon, Portugal.
- Sadek, F., Mohraz, B., Taylor, A.W. and Chung, R.M. (1997), “A method of estimating the parameters of tuned mass dampers for seismic applications”, *Earthq. Eng. Struct. Dyn.*, **26**, 617-635.
- Schmitendorf, W.E. (2000), “Designing tuned mass dampers via static output feedback: A numerical approach”, *Earthq. Eng. Struct. Dyn.*, **29**, 127-137.
- Singh, M.P., Singh, S. and Moreschi, L.M. (2002), “Tuned mass dampers for response control of torsional buildings”, *Earthq. Eng. Struct. Dyn.*, **31**, 749-769.
- Soong, T.T. and Dargush, G.F. (1997), *Passive Energy Dissipation Systems in Structural Engineering*, John Wiley & Sons Ltd., Chichester.
- Takewaki, I. (1997), “Optimal damper placement for minimum transfer functions”, *Earthq. Eng. Struct. Dyn.*, **26**(11), 1113-1124.
- Takewaki, I. (2000a), “Soil-structure random response reduction via TMD-VD simultaneous use”, *Comput. Meth. Appl. Mech. Eng.*, **190**, 677-690.
- Takewaki, I. (2000b), “Optimal damper placement for planar building frames using transfer functions”, *Struct. Multidiscip. O.*, **20**(4), 280-287.
- Takewaki, I., Yoshitomi, S., Uetani, K. and Tsuji, M. (1999), “Non-monotonic optimal damper placement via steepest direction search”, *Earthq. Eng. Struct. Dyn.*, **28**(6), 655-670.
- Tso, W.K. and Yao, S. (1994), “Seismic load distribution in buildings with eccentric setback”, *Can. J. Civil Eng.*, **21**, 50-62.
- Venanzi, I., Ubertini, F. and Materazzi, A.L. (2013), “Optimal design of an array of active tuned mass dampers for wind-exposed high-rise buildings”, *Struct. Control Hlth. Monit.*, **20**, 903-917.
- Warburton, G.B. (1982), “Optimum absorber parameters for various combinations of response and excitation parameters”, *Earthq. Eng. Struct. Dyn.*, **10**, 381-401.
- Wang, J.F., Lin, C.C. and Lian, C.H. (2009), “Two-stage optimum design of tuned mass dampers with consideration of stroke”, *Struct. Control Hlth. Monit.*, **16**, 55-72.
- Wiesner, K.B. (1979), “Tuned mass dampers to reduce building wind motion”, *ASCE Convention and Exposition*, Boston, Mass, 1-21.
- Wirsching, P.H. and Campbell, G.W. (1974), “Minimal structural response under random excitations using vibration absorber”, *Earthq. Eng. Struct. Dyn.*, **2**, 303-312.
- Zuo, L. and Nayfeh, S.A. (2004), “Minimax optimization of multi-degree-of-freedom tuned-mass dampers”, *J. Sound Vib.*, **272**, 893-908.

Appendix

Appendix A: KKT conditions derivation

For an optimization problem with the following form

$$\begin{aligned}
 & \min_{\mathbf{x}} f(\mathbf{x}) \\
 & s.t. \quad g_i(\mathbf{x}) \leq 0 \quad \forall i = 1, \dots, m \\
 & \quad \quad h_j(\mathbf{x}) = 0 \quad \forall j = 1, \dots, n
 \end{aligned} \tag{A1}$$

a solution \mathbf{x}^* is called a Karush–Kuhn–Tucker (KKT) point if it fulfills the following conditions (see for example, Bazaraa and Shetty 1979)

$$\begin{aligned}
 (1) \quad & \nabla f(\mathbf{x}^*) + \sum_{i=1}^m \lambda_i \cdot \nabla g_i(\mathbf{x}^*) + \sum_{j=1}^n \mu_j \cdot \nabla h_j(\mathbf{x}^*) = \mathbf{0} \\
 (2) \quad & \lambda_i \cdot g_i(\mathbf{x}^*) = 0 \quad \forall i = 1, \dots, m \\
 (3) \quad & \lambda_i \geq 0 \quad \forall i = 1, \dots, m \\
 (4) \quad & g_i(\mathbf{x}^*) \leq 0 \quad \forall i = 1, \dots, m \\
 (5) \quad & h_j(\mathbf{x}^*) = 0 \quad \forall j = 1, \dots, n
 \end{aligned} \tag{A2}$$

Where ∇ represents the gradient of a function, λ and μ represent Lagrange multipliers. In a convex problem, a KKT point is necessarily a local as well as a global optimum. In other problems, a local minimum will either fulfill the KKT conditions, or be an irregular solution for which the vectors $\{\nabla g_i(\mathbf{x}^*) | g_i(\mathbf{x}^*) = 0\}_{i=1}^m$ and $\{\nabla h_j(\mathbf{x}^*)\}_{j=1}^n$ are linearly-dependent.

In accordance to Eq. (A4), the optimization problem (Eq. (1)) is formulated such that

$$\begin{aligned}
 \min J &= \sum_l^{\text{all locations}} \sum_f^{\text{all frequencies}} (\mathbf{m}_{TMD})_{l,f} \\
 s.t. \quad & RMS\left(\left(\ddot{\mathbf{x}}_p^t\right)_l\right) - a_{\text{all}}^{\text{RMS}} \leq 0 \quad \forall l = 1, 2, \dots, N_{\text{locations}} \\
 & -(\mathbf{m}_{TMD})_{l,f} \leq 0 \quad \forall l = 1, 2, \dots, N_{\text{locations}}; \quad \forall f = 1, 2, \dots, N_{\text{mode}}
 \end{aligned} \tag{A3}$$

for which the KKT conditions are

$$\begin{aligned}
& (1) \lambda_1 \cdot \left\{ \begin{array}{c} \frac{\partial RMS(\ddot{\mathbf{x}}_p^t)}{\partial (\mathbf{m}_{TMD})_{1,1}} \\ \vdots \\ \frac{\partial RMS(\ddot{\mathbf{x}}_p^t)}{\partial (\mathbf{m}_{TMD})_{N_{locations}, N_{mode}}} \end{array} \right\} + \lambda_2 \cdot \left\{ \begin{array}{c} \frac{\partial RMS(\ddot{\mathbf{x}}_p^t)}{\partial (\mathbf{m}_{TMD})_{1,1}} \\ \vdots \\ \frac{\partial RMS(\ddot{\mathbf{x}}_p^t)}{\partial (\mathbf{m}_{TMD})_{N_{locations}, N_{mode}}} \end{array} \right\} + \dots + \lambda_{N_{locations}} \cdot \left\{ \begin{array}{c} \frac{\partial RMS(\ddot{\mathbf{x}}_p^t)}{\partial (\mathbf{m}_{TMD})_{1,1}} \\ \vdots \\ \frac{\partial RMS(\ddot{\mathbf{x}}_p^t)}{\partial (\mathbf{m}_{TMD})_{N_{locations}, N_{mode}}} \end{array} \right\} + \\
& \beta_{1,2} \cdot \left\{ \begin{array}{c} -1 \\ 0 \\ \vdots \\ 0 \end{array} \right\} + \beta_{2,1} \cdot \left\{ \begin{array}{c} 0 \\ -1 \\ 0 \\ \vdots \\ 0 \end{array} \right\} + \dots + \beta_{N_{locations}, N_{mode}} \cdot \left\{ \begin{array}{c} 0 \\ 0 \\ \vdots \\ -1 \end{array} \right\} + = \left\{ \begin{array}{c} -1 \\ -1 \\ \vdots \\ -1 \end{array} \right\} \\
& (2) \lambda_l \cdot (RMS(\ddot{\mathbf{x}}_p^t) - a_{all}^{RMS}) = 0 \quad \forall l = 1, 2, \dots, N_{locations} \\
& \quad \beta_{l,f} \cdot (-\mathbf{m}_{TMD})_{l,f} = 0 \quad \forall l = 1, 2, \dots, N_{locations}; \quad \forall f = 1, 2, \dots, N_{mode} \\
& (3) \lambda_l \geq 0 \quad \forall l = 1, 2, \dots, N_{locations} \\
& \quad \beta_{l,f} \geq 0 \quad \forall l = 1, 2, \dots, N_{locations}; \quad \forall f = 1, 2, \dots, N_{mode} \\
& (4) RMS(\ddot{\mathbf{x}}_p^t) - a_{all}^{RMS} \leq 0 \quad \forall l = 1, 2, \dots, N_{locations} \\
& \quad -\mathbf{m}_{TMD})_{l,f} \leq 0 \quad \forall l = 1, 2, \dots, N_{locations}; \quad \forall f = 1, 2, \dots, N_{mode}
\end{aligned} \tag{A4}$$

For the sake of demonstration let us consider a two story structure ($N_{locations} = 2$) for which in each floor, two dampers are potentially added, to suppress two frequencies of the structure ($N_{mode} = 2$). Thus now the KKT conditions in Eq. (A4) must follow

$$\begin{aligned}
& (1) \lambda_1 \cdot \left\{ \begin{array}{c} \frac{\partial RMS(\ddot{\mathbf{x}}_p^t)}{\partial (\mathbf{m}_{TMD})_{1,1}} \\ \frac{\partial RMS(\ddot{\mathbf{x}}_p^t)}{\partial (\mathbf{m}_{TMD})_{2,1}} \\ \frac{\partial RMS(\ddot{\mathbf{x}}_p^t)}{\partial (\mathbf{m}_{TMD})_{1,2}} \\ \frac{\partial RMS(\ddot{\mathbf{x}}_p^t)}{\partial (\mathbf{m}_{TMD})_{2,2}} \end{array} \right\} + \lambda_2 \cdot \left\{ \begin{array}{c} \frac{\partial RMS(\ddot{\mathbf{x}}_p^t)}{\partial (\mathbf{m}_{TMD})_{1,1}} \\ \frac{\partial RMS(\ddot{\mathbf{x}}_p^t)}{\partial (\mathbf{m}_{TMD})_{2,1}} \\ \frac{\partial RMS(\ddot{\mathbf{x}}_p^t)}{\partial (\mathbf{m}_{TMD})_{1,2}} \\ \frac{\partial RMS(\ddot{\mathbf{x}}_p^t)}{\partial (\mathbf{m}_{TMD})_{2,2}} \end{array} \right\} + \beta_{1,1} \cdot \left\{ \begin{array}{c} -1 \\ 0 \\ 0 \\ 0 \end{array} \right\} + \beta_{2,1} \cdot \left\{ \begin{array}{c} 0 \\ -1 \\ 0 \\ 0 \end{array} \right\} + \beta_{1,2} \cdot \left\{ \begin{array}{c} 0 \\ 0 \\ -1 \\ 0 \end{array} \right\} + \beta_{2,2} \cdot \left\{ \begin{array}{c} 0 \\ 0 \\ 0 \\ -1 \end{array} \right\} = \left\{ \begin{array}{c} -1 \\ -1 \\ -1 \\ -1 \end{array} \right\}
\end{aligned} \tag{A5}$$

$$\begin{aligned}
 (2) \quad & \lambda_1 \cdot \left(RMS(\ddot{\mathbf{x}}_p^t)_1 - a_{\text{all}}^{\text{RMS}} \right) = 0 \\
 & \lambda_2 \cdot \left(RMS(\ddot{\mathbf{x}}_p^t)_2 - a_{\text{all}}^{\text{RMS}} \right) = 0 \\
 & \beta_{1,1} \cdot \left(-(\mathbf{m}_{TMD})_{1,1} \right) = 0 \\
 & \beta_{2,1} \cdot \left(-(\mathbf{m}_{TMD})_{2,1} \right) = 0 \\
 & \beta_{1,2} \cdot \left(-(\mathbf{m}_{TMD})_{1,2} \right) = 0 \\
 & \beta_{2,2} \cdot \left(-(\mathbf{m}_{TMD})_{2,2} \right) = 0 \\
 (3) \quad & \lambda_l \geq 0 \quad \forall l = 1, 2 \\
 & \beta_{l,f} \geq 0 \quad \forall l = 1, 2; \forall f = 1, 2 \\
 (4) \quad & RMS(\ddot{\mathbf{x}}_p^t)_1 - a_{\text{all}}^{\text{RMS}} \leq 0 \\
 & RMS(\ddot{\mathbf{x}}_p^t)_2 - a_{\text{all}}^{\text{RMS}} \leq 0 \\
 & -(\mathbf{m}_{TMD})_{l,f} \leq 0 \quad \forall l = 1, 2; \forall f = 1, 2
 \end{aligned}$$

For derivation of the KKT conditions, an assumption is made that at the optimal solution, only one constraint is active (i.e., only the acceleration at one location equals the allowable, while the other accelerations are all smaller than the allowable). However, it was seen in various examples that even if more than one acceleration has reached the allowable, the solution obtained using these KKT conditions and the analysis/redesign scheme, is close to the actual optimal solution to the problem.

Under the assumption that only one constraint is active at the optimum, λ_l of all locations, other than that of the location where the constraint is active, equal zero (based on (2) in the KKT conditions). Thus, the vector of gradients that multiply this factor is of no significance to the KKT conditions. Let us assume that for the 2 story example, the acceleration at the second floor equals the allowable, while that of the first floor is smaller than the allowable. Therefore: $\lambda_1 = 0$; $\lambda_2 > 0$.

This leads to

$$(1) \quad \lambda_2 \cdot \left\{ \begin{array}{l} \frac{\partial RMS(\ddot{\mathbf{x}}_p^t)_2}{\partial (\mathbf{m}_{TMD})_{1,1}} \\ \frac{\partial RMS(\ddot{\mathbf{x}}_p^t)_2}{\partial (\mathbf{m}_{TMD})_{2,1}} \\ \frac{\partial RMS(\ddot{\mathbf{x}}_p^t)_2}{\partial (\mathbf{m}_{TMD})_{1,2}} \\ \frac{\partial RMS(\ddot{\mathbf{x}}_p^t)_2}{\partial (\mathbf{m}_{TMD})_{2,2}} \end{array} \right\} + \beta_{1,1} \cdot \left\{ \begin{array}{l} -1 \\ 0 \\ 0 \\ 0 \end{array} \right\} + \beta_{2,1} \cdot \left\{ \begin{array}{l} 0 \\ -1 \\ 0 \\ 0 \end{array} \right\} + \beta_{1,2} \cdot \left\{ \begin{array}{l} 0 \\ 0 \\ -1 \\ 0 \end{array} \right\} + \beta_{2,2} \cdot \left\{ \begin{array}{l} 0 \\ 0 \\ 0 \\ -1 \end{array} \right\} = \left\{ \begin{array}{l} -1 \\ -1 \\ -1 \\ -1 \end{array} \right\} \quad (A6)$$

Based on Eq. (A5) and noting that $\lambda_2 > 0$ and $\beta_{l,f} \geq 0$ (from the KKT conditions in Eq. (A2)), it could be observed that if a certain $\beta_{l,f}$ equals zero, the value of the gradient corresponding to that $\beta_{l,f}$, i.e. $\frac{\partial RMS(\{\{\dot{\mathbf{x}}_p^t\}_2)}{\partial (\mathbf{m}_{TMD})_{l,f}}$, has to be most negative of all gradient entries that multiply λ_2 . This is since the value of λ_2 is positive, and will be determined by the equation corresponding to the line where the vector multiplying $\beta_{l,f} = 0$ equals minus 1. Now, since all other $\beta_{l,f}$ are positive, and λ_2 has been determined, the gradient values corresponding to these $\beta_{l,f}$ must obtain a less negative value in order to satisfy their corresponding equations in Eq. (A5). Note that $\beta_{l,f} = 0$ only where corresponding masses obtain values larger than zero. Furthermore, if more than one $\beta_{l,f}$ equals zero, it could be observed, from the corresponding lines in condition (1), that their values should be equal and most negative. This is since they are multiplied by the same value of λ_2 . In summary, the KKT condition that is obtained (under the assumption that only one constraint is active), and then used as the basis of step 2 of the analysis/redesign procedure, is that at any location and frequency where there are dampers, the gradient of the constraint at that location with respect to masses that have values other than zero (at the optimal solution) are equal and most negative.

Appendix B: approximate gradient derivation

As can be seen in the derivation for the KKT conditions in Appendix A, the gradients of the constraints with respect to the different design variables (masses) are used. These gradients may be derived in an analytical manner. However, this may be rather excruciating for engineers to use. Therefore, in this paper, an approximated gradient is derived. The expression for the approximate gradient is simple, and can be used together with the analysis/redesign scheme presented above, to result in a computationally simple design methodology. To obtain the approximated expression, several assumptions are made. Those will be explained within the following derivation. Appendix B1 presents a transformation of the Multi Degree-Of-Freedom (MDOF) system to a set of SDOF systems. Then, in appendix B2, an approximated gradient is derived based on the SDOF systems and their contributions to the MDOF response.

Appendix B1: derivation of equivalent SDOF systems

For a MDOF structural system with MTMDs under seismic input, the equations of motion can be formulated in the following manner

$$\begin{aligned} & (\mathbf{M}_{\text{original}} + \mathbf{B}_{\text{dm}}^T \mathcal{D}(\{\mathbf{m}_{\text{TMD}}\}) \mathbf{B}_{\text{dm}}) \ddot{\mathbf{x}} + \mathbf{C}_{\text{original}} \dot{\mathbf{x}} + \mathbf{K}_{\text{original}} \mathbf{x} = \\ & - \mathbf{M}_{\text{original}} \mathbf{e}_s a_g + \mathbf{B}_d^T \mathcal{D}(\mathbf{c}_{\text{TMD}}) \dot{\mathbf{z}} + \mathbf{B}_d^T \mathcal{D}(\mathbf{k}_{\text{TMD}}) \mathbf{z} \end{aligned} \quad (\text{A7})$$

where $\mathbf{M}_{\text{original}}$ is the mass matrix of the structure, $\mathbf{C}_{\text{original}}$ is the inherent damping matrix of the structure, $\mathbf{K}_{\text{original}}$ is the stiffness matrix of the structure, $\ddot{\mathbf{x}}$, $\dot{\mathbf{x}}$ and \mathbf{x} are the structure's acceleration, velocity and displacement relative to the ground, respectively. \mathbf{e}_s is the influence

vector (of the structure), \mathbf{a}_g is the ground motion acceleration, \mathbf{m}_{TMD} is the TMDs' mass vector, \mathbf{C}_{TMD} is the TMDs' inherent damping vector, \mathbf{k}_{TMD} is the TMDs' stiffness vector, the matrix \mathbf{B}_d is a transformation matrix, used to assign the TMDs within the structure, the matrix \mathbf{B}_{dm} is a transformation matrix, used to account for the addition of mass in the direction of which the TMDs do not move, and $\dot{\mathbf{z}}$ and \mathbf{z} are the TMD's velocity and displacement relative to the structure (in the same peripheral location), respectively. $\mathcal{D}(\cdot)$ turns a vector (\cdot) into a diagonal matrix with its elements on the diagonal.

As for the equations of motion of the TMDs, those can be formulated as

$$\mathcal{D}(\mathbf{m}_{\text{TMD}})\ddot{\mathbf{z}} + \mathcal{D}(\mathbf{c}_{\text{TMD}})\dot{\mathbf{z}} + \mathcal{D}(\mathbf{k}_{\text{TMD}})\mathbf{z} = -\mathcal{D}(\mathbf{m}_{\text{TMD}})\mathbf{B}_d\ddot{\mathbf{x}} - \mathcal{D}(\mathbf{m}_{\text{TMD}})\cdot\mathbf{e}_d\mathbf{a}_g \quad (\text{A8})$$

where $\ddot{\mathbf{z}}$ is the TMDs' acceleration relative to the structure.

Assuming behavior based on a certain mode, displacements are expressed as

$$\mathbf{x} = \phi_f x_{\text{max}} \quad (\text{A9})$$

where x_{max} is the displacement where the mode shape ϕ_f is normalized to 1.0. Placing this expression into Eq. (A7) and Eq. (A8), and assuming that the forces acting on the TMDs (last term on right hand side of Eq. (A8)) is negligible, gives

$$\begin{aligned} & (\mathbf{M}_{\text{original}} + \mathbf{B}_{dm}^T \mathcal{D}(\mathbf{m}_{\text{TMD}})\mathbf{B}_{dm})\phi_f \ddot{x}_{\text{max}} + \mathbf{C}_{\text{original}}\phi_f \dot{x}_{\text{max}} + \mathbf{K}_{\text{original}}\phi_f x_{\text{max}} = \\ & -\mathbf{M}_{\text{original}}\mathbf{e}_s\mathbf{a}_g + \mathbf{B}_d^T \mathcal{D}(\mathbf{c}_{\text{TMD}})\dot{\mathbf{z}} + \mathbf{B}_d^T \mathcal{D}(\mathbf{k}_{\text{TMD}})\mathbf{z} \end{aligned} \quad (\text{A10})$$

and

$$\mathcal{D}(\mathbf{m}_{\text{TMD}})\ddot{\mathbf{z}} + \mathcal{D}(\mathbf{c}_{\text{TMD}})\dot{\mathbf{z}} + \mathcal{D}(\mathbf{k}_{\text{TMD}})\mathbf{z} = -\mathcal{D}(\mathbf{m}_{\text{TMD}})\mathbf{B}_d\phi_f \ddot{x}_{\text{max}} \quad (\text{A11})$$

Normalizing Eq. (A11) by the TMDs masses yields

$$\mathbf{I}\ddot{\mathbf{z}} + \mathbf{I}2\xi_j\omega_j\dot{\mathbf{z}} + \mathbf{I}\omega_j^2\mathbf{z} = -\mathbf{B}_d\phi_f \ddot{x}_{\text{max}} \quad (\text{A12})$$

It can be seen from Eq. (A12) that \mathbf{z} is proportional to $\mathbf{B}_d\phi_f$. Therefore, it can be written as

$$\mathbf{z} = \mathbf{B}_d\phi_f z_{\text{max}} \quad (\text{A13})$$

where z_{max} is the value of z in the same location where x is maximal, normalized by $\mathbf{B}_d\phi_f$ at that location. Substituting Eq. (A13) into Eq. (A11) gives

$$\mathcal{D}(\mathbf{m}_{\text{TMD}})\mathbf{B}_d\phi_f \ddot{z}_{\text{max}} + \mathcal{D}(\mathbf{c}_{\text{TMD}})\dot{\mathbf{z}} + \mathcal{D}(\mathbf{k}_{\text{TMD}})\mathbf{z} = -\mathcal{D}(\mathbf{m}_{\text{TMD}})\mathbf{B}_d\phi_f \ddot{x}_{\text{max}} \quad (\text{A14})$$

and therefore

$$\mathcal{D}(\mathbf{c}_{\text{TMD}})\dot{\mathbf{z}} + \mathcal{D}(\mathbf{k}_{\text{TMD}})\mathbf{z} = -\mathcal{D}(\mathbf{m}_{\text{TMD}})\mathbf{B}_d\phi_f (\ddot{z}_{\text{max}} + \ddot{x}_{\text{max}}) \quad (\text{A15})$$

Substituting Eq. (A14) in Eq. (A10) yields

$$\begin{aligned} & \left(\mathbf{M}_{\text{original}} + \mathbf{B}_{\text{dm}}^T \mathcal{D}(\mathbf{m}_{\text{TMD}}) \mathbf{B}_{\text{dm}} \right) \phi_f \ddot{x}_{\text{max}} + \mathbf{C}_{\text{original}} \phi_f \dot{x}_{\text{max}} + \mathbf{K}_{\text{original}} \phi_f x_{\text{max}} = \\ & - \mathbf{M}_{\text{original}} \mathbf{e}_s a_g - \mathbf{B}_{\text{d}}^T \mathcal{D}(\mathbf{m}_{\text{TMD}}) \mathbf{B}_{\text{d}} \phi_f (\ddot{z}_{\text{max}} + \ddot{x}_{\text{max}}) \end{aligned} \quad (\text{A16})$$

Substituting Eq. (A13) in Eq. (A14) yields

$$\begin{aligned} & \mathcal{D}(\mathbf{m}_{\text{TMD}}) \mathbf{B}_{\text{d}} \phi_f \ddot{z}_{\text{max}} + \mathcal{D}(\mathbf{c}_{\text{TMD}}) \mathbf{B}_{\text{d}} \phi_f \dot{z}_{\text{max}} + \mathcal{D}(\mathbf{k}_{\text{TMD}}) \mathbf{B}_{\text{d}} \phi_f z_{\text{max}} = \\ & - \mathcal{D}(\mathbf{m}_{\text{TMD}}) \mathbf{B}_{\text{d}} \phi_f \ddot{x}_{\text{max}} \end{aligned} \quad (\text{A17})$$

Multiplying Eq. (A16) by ϕ_f^T on the left and Eq. (A17) by $\phi_f^T \mathbf{B}_{\text{d}}^T$ on the left, turns them into

$$\begin{aligned} & \phi_f^T \left(\mathbf{M}_{\text{original}} + \mathbf{B}_{\text{dm}}^T \mathcal{D}(\mathbf{m}_{\text{TMD}}) \mathbf{B}_{\text{dm}} \right) \phi_f \ddot{x}_{\text{max}} + \phi_f^T \mathbf{C}_{\text{original}} \phi_f \dot{x}_{\text{max}} + \phi_f^T \mathbf{K}_{\text{original}} \phi_f x_{\text{max}} = \\ & - \phi_f^T \mathbf{M}_{\text{original}} \mathbf{e}_s a_g - \phi_f^T \mathbf{B}_{\text{d}}^T \mathcal{D}(\mathbf{m}_{\text{TMD}}) \mathbf{B}_{\text{d}} \phi_f (\ddot{z}_{\text{max}} + \ddot{x}_{\text{max}}) \end{aligned} \quad (\text{A18})$$

and

$$\begin{aligned} & \phi_f^T \mathbf{B}_{\text{d}}^T \mathcal{D}(\mathbf{m}_{\text{TMD}}) \mathbf{B}_{\text{d}} \phi_f \ddot{z}_{\text{max}} + \phi_f^T \mathbf{B}_{\text{d}}^T \mathcal{D}(\mathbf{c}_{\text{TMD}}) \mathbf{B}_{\text{d}} \phi_f \dot{z}_{\text{max}} + \\ & \phi_f^T \mathbf{B}_{\text{d}}^T \mathcal{D}(\mathbf{k}_{\text{TMD}}) \mathbf{B}_{\text{d}} \phi_f z_{\text{max}} = - \phi_f^T \mathbf{B}_{\text{d}}^T \mathcal{D}(\mathbf{m}_{\text{TMD}}) \mathbf{B}_{\text{d}} \phi_f \ddot{x}_{\text{max}} \end{aligned} \quad (\text{A19})$$

Eq. (A18) and Eq. (A19) can be written in short as

$$M_f \ddot{x}_{\text{max}} + C_f \dot{x}_{\text{max}} + K_f x_{\text{max}} = - \phi_f^T \mathbf{M}_{\text{original}} \mathbf{e}_s a_g - m_f (\ddot{z}_{\text{max}} + \ddot{x}_{\text{max}}) \quad (\text{A20})$$

and

$$m_f \ddot{z}_{\text{max}} + c_f \dot{z}_{\text{max}} + k_f z_{\text{max}} = - m_f \ddot{x}_{\text{max}} \quad (\text{A21})$$

where

$$\begin{aligned} M_f &= \phi_f^T \left(\mathbf{M}_{\text{original}} + \mathbf{B}_{\text{dm}}^T \mathcal{D}(\mathbf{m}_{\text{TMD}}) \mathbf{B}_{\text{dm}} \right) \phi_f \\ C_f &= \phi_f^T \mathbf{C}_{\text{original}} \phi_f \\ K_f &= \phi_f^T \mathbf{K}_{\text{original}} \phi_f \\ m_f &= \phi_f^T \mathbf{B}_{\text{d}}^T \mathcal{D}(\mathbf{m}_{\text{TMD}}) \mathbf{B}_{\text{d}} \phi_f \\ c_f &= \phi_f^T \mathbf{B}_{\text{d}}^T \mathcal{D}(\mathbf{c}_{\text{TMD}}) \mathbf{B}_{\text{d}} \phi_f \\ k_f &= \phi_f^T \mathbf{B}_{\text{d}}^T \mathcal{D}(\mathbf{k}_{\text{TMD}}) \mathbf{B}_{\text{d}} \phi_f \end{aligned} \quad (\text{A22})$$

Eq. (A20) and Eq. (A21) are two SDOF equations (i.e., one DOF of the structure and one of the TMDs). For this equivalent SDOF system

$$\begin{aligned} (\boldsymbol{\mu}_{\text{TMD}})_f &= \frac{m_f}{M_f} \\ (\boldsymbol{\omega}_n)_f &= \sqrt{\frac{K_f}{M_f}} \end{aligned} \quad (\text{A23})$$

Based on these definitions, Eq. (A20) can be normalized in the following manner, to represent each of the equivalent SDOF systems

$$\ddot{x}_{\text{max}} + 2\xi_f \omega_f \dot{x}_{\text{max}} + \omega_f^2 x_{\text{max}} = -\Gamma_f a_g - \mu_f (\ddot{z}_{\text{max}} + \ddot{x}_{\text{max}}) \quad (\text{A24})$$

where $\Gamma_f = \phi_f^T \mathbf{M}_{\text{original}} \mathbf{e}_s / M_f$.

Appendix B2: Derivation of approximate gradient

Under the same assumptions that apply to SRSS (square-root of sum of squares) derivation, it can be shown that a mean square response can be represented by the sum of mean-square (MS) of modal contributions to a specific response, such that

$$MS\left(\left(\ddot{\mathbf{x}}_p^t\right)_l\right) \cong \sum_{f=\text{relevant modes}} MS_f\left(\left(\ddot{\mathbf{x}}_p^t\right)_l\right) \quad (\text{A25})$$

The contribution of mode f to the mean-square response at a specific location can be shown to be

$$MS_f\left(\left(\ddot{\mathbf{x}}_p^t\right)_l\right) = (\mathbf{T} \cdot \phi_f)_l^2 \Gamma_f^2 MS\left(\ddot{\mathbf{x}}_p^t\right)_{\text{max}} \quad (\text{A26})$$

Substituting Eq. (A26) into Eq. (A25) and taking the root leads to the following root-mean-square (RMS) acceleration at location l at iteration cycle n

$$\begin{aligned} RMS\left(\left(\ddot{\mathbf{x}}_p^t\right)_l\right) &= \\ &= \sqrt{2 \cdot \left((\mathbf{T} \cdot \phi_1)_l^2 \cdot \Gamma_1^2 \cdot MS\left(\ddot{\mathbf{x}}_p^t(\omega_1)\right)_{\text{max}} + (\mathbf{T} \cdot \phi_2)_l^2 \cdot \Gamma_2^2 \cdot MS\left(\ddot{\mathbf{x}}_p^t(\omega_2)\right)_{\text{max}} + \dots \right)} \end{aligned} \quad (\text{A27})$$

for which the derivative with respect to the design variables (masses) is

$$\begin{aligned} \frac{\partial \left(RMS\left(\left(\ddot{\mathbf{x}}_p^t\right)_l\right) \right)}{\partial (\mathbf{m}_{\text{TMD}})_{l,f}} &= \frac{1}{2 \cdot RMS\left(\left(\ddot{\mathbf{x}}_p^t\right)_l\right)} \cdot 2 \cdot (\mathbf{T} \cdot \phi_f)_l^2 \cdot \Gamma_f^2 \cdot \frac{\partial \left(MS\left(\ddot{\mathbf{x}}_p^t(\omega_f)\right)_{\text{max}} \right)}{\partial (\mathbf{m}_{\text{TMD}})_{l,f}} = \\ &= \frac{(\mathbf{T} \cdot \phi_f)_l^2 \cdot \Gamma_f^2}{RMS\left(\left(\ddot{\mathbf{x}}_p^t\right)_l\right)} \cdot \frac{\partial \left(MS\left(\ddot{\mathbf{x}}_p^t(\omega_f)\right)_{\text{max}} \right)}{\partial (\boldsymbol{\mu}_{\text{TMD}})_f} \cdot \frac{\partial (\boldsymbol{\mu}_{\text{TMD}})_f}{\partial (\mathbf{m}_{\text{TMD}})_{l,f}} \end{aligned} \quad (\text{A28})$$

and the derivative $\frac{\partial (\boldsymbol{\mu}_{\text{TMD}})_f}{\partial (\mathbf{m}_{\text{TMD}})_{l,f}}$ (in a 3D frame, based on Eq. (A23)) is

$$\frac{\partial(\boldsymbol{\mu}_{\text{TMD}})_f}{\partial(\mathbf{m}_{\text{TMD}})_{l,f}} = \frac{\phi_f^T \mathbf{B}_d^T \frac{\partial \mathcal{D}(\mathbf{m}_{\text{TMD}})}{\partial(\mathbf{m}_{\text{TMD}})_{l,f}} \mathbf{B}_d \phi_f}{\phi_f^T \cdot \mathbf{M}_f \cdot \phi_f} \quad (\text{A29})$$

Therefore

$$\frac{\partial \left(\text{RMS} \left(\left(\ddot{\mathbf{x}}_p^t(n) \right)_l \right) \right)}{\partial(\mathbf{m}_{\text{TMD}})_{l,f}} \approx \frac{(\mathbf{T} \cdot \phi_f)_l^2 \cdot \Gamma_f^2}{\text{RMS} \left(\left(\ddot{\mathbf{x}}_p^t(n) \right)_l \right)} \cdot \frac{\phi_f^T \mathbf{B}_d^T \frac{\partial \mathcal{D}(\mathbf{m})}{\partial(\mathbf{m}_{\text{TMD}})_{l,f}} \mathbf{B}_d \phi_f}{\phi_f^T \cdot \mathbf{M}_f \cdot \phi_f} \cdot \frac{\partial \left(MS \left(\left(\ddot{\mathbf{x}}_p^t(\omega_f)^n \right)_{\max} \right) \right)}{\partial(\boldsymbol{\mu}_{\text{TMD}})_f} \quad (\text{A30})$$

where $\frac{\partial(a_{MS}(\omega_f)_{\max})}{\partial(\boldsymbol{\mu}_{\text{TMD}})_f}$ is obtained based on a SDOF equivalent system for that mode, using the

following empiric formula, that was obtained based on curve-fitting techniques

$$\frac{\partial \left(MS \left(\left(\ddot{\mathbf{x}}_p^t(\omega_f)^n \right)_{\max} \right) \right)}{\partial(\boldsymbol{\mu}_{\text{TMD}})_f} = -3.15099 \cdot \left((\boldsymbol{\mu}_{\text{TMD}})_f + 0.003 \right)^{-1.12041} \cdot \left((\boldsymbol{\omega}_n)_f \right)^{0.5} \cdot S \left((\boldsymbol{\omega}_n)_f \right) \quad (\text{A31})$$